Cell Reports

Report

Rapamycin Reverses Metabolic Deficits in Lamin A/C-Deficient Mice

Graphical Abstract

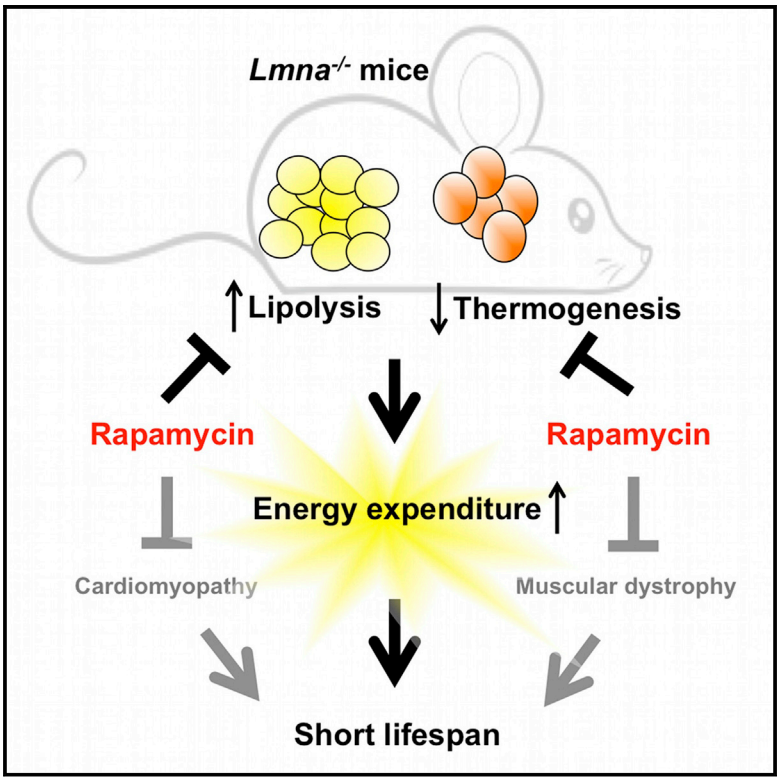

Authors

Chen-Yu Liao, Sydney S. Anderson, Nicole H. Chicoine, ..., Mark A. McCormick, Monique N. O'Leary, Brian K. Kennedy

Correspondence

bkennedy@buckinstitute.org

In Brief

Liao et al. find that lifespan extension by rapamycin is associated with suppression of elevated energy expenditure in *Lmna*$^{-/-}$ mice, a model for lipodystrophy. Molecularly, rapamycin suppresses elevated lipolysis and restores the levels of the thermogenic protein, UCP1. The metabolic phenotypes of *Lmna*$^{-/-}$ mice can also be partially rescued by maintaining mice at thermoneutrality.

Highlights

- Rapamycin suppresses the elevated energy expenditure in *Lmna*$^{-/-}$ mice
- Rapamycin suppresses elevated lipolysis of white adipose tissue in *Lmna*$^{-/-}$ mice
- Rapamycin restores the thermogenic protein UCP1 levels in *Lmna*$^{-/-}$ mice
- Thermoneutrality partially rescues the metabolic phenotypes of *Lmna*$^{-/-}$ mice

Liao et al., 2016, Cell Reports *17*, 2542–2552
December 6, 2016
http://dx.doi.org/10.1016/j.celrep.2016.10.040

CellPress

OPEN ACCESS
CellPress

Cell Reports
Report

Rapamycin Reverses Metabolic Deficits in Lamin A/C-Deficient Mice

Chen-Yu Liao,[1] Sydney S. Anderson,[1] Nicole H. Chicoine,[1] Jarrott R. Mayfield,[1] Emmeline C. Academia,[1] Joy A. Wilson,[1] Chalermkwan Pongkietisak,[1] Morgan A. Thompson,[1] Earl P. Lagmay,[1] Delana M. Miller,[1] Yueh-Mei Hsu,[1] Mark A. McCormick,[1] Monique N. O'Leary,[1,2] and Brian K. Kennedy[1,3,*]

[1]Buck Institute for Research on Aging, 8001 Redwood Blvd., Novato, CA 94945, USA
[2]Current Address: University of Michigan, Department of Pathology, 109 Zina Pitcher Place, Ann Arbor, MI 48109
[3]Lead Contact
*Correspondence: bkennedy@buckinstitute.org
http://dx.doi.org/10.1016/j.celrep.2016.10.040

SUMMARY

The role of the mTOR inhibitor, rapamycin, in regulation of adiposity remains controversial. Here, we evaluate mTOR signaling in lipid metabolism in adipose tissues of *Lmna*$^{-/-}$ mice, a mouse model for dilated cardiomyopathy and muscular dystrophy. Lifespan extension by rapamycin is associated with increased body weight and fat content, two phenotypes we link to suppression of elevated energy expenditure. In both white and brown adipose tissue of *Lmna*$^{-/-}$ mice, we find that rapamycin inhibits mTORC1 but not mTORC2, leading to suppression of elevated lipolysis and restoration of thermogenic protein UCP1 levels, respectively. The short lifespan and metabolic phenotypes of *Lmna*$^{-/-}$ mice can be partially rescued by maintaining mice at thermoneutrality. Together, our findings indicate that altered mTOR signaling in *Lmna*$^{-/-}$ mice leads to a lipodystrophic phenotype that can be rescued with rapamycin, highlighting the effect of loss of adipose tissue in *Lmna*$^{-/-}$ mice and the consequences of altered mTOR signaling.

INTRODUCTION

The mechanistic target of rapamycin (mTOR) protein is well known to orchestrate cell growth and proliferation (Laplante and Sabatini, 2012) and is linked to a range of age-related diseases (Johnson et al., 2013a). Rapamycin, which inhibits mTOR signaling, prolongs the lifespan in a variety of genetically different mice (Anisimov et al., 2011; Harrison et al., 2009; Neff et al., 2013) and genetically modified mouse models of various human diseases (Fujishita et al., 2008; Johnson et al., 2013b; Ramos et al., 2012).

Accumulating evidence also indicates that mTOR complex 1 (mTORC1) plays a key role in the regulation of fat metabolism (Cai et al., 2016; Lamming and Sabatini, 2013). Upon activation, mTORC1 suppresses lipolytic enzymes, represses lipolysis, and activates lipogenesis and lipid storage, whereas inhibition of mTORC1 blocks adipogenesis and stimulates lipolysis (Chakrabarti et al., 2010; Lamming and Sabatini, 2013). In light of this, rapamycin, which is known to acutely inhibit mTORC1, has been shown to suppress the adiposity and/or body weight (BW) of mice (Anisimov et al., 2011; Fang et al., 2013; Miller et al., 2014). Genetic interventions leading to mTORC1 inhibition, such as adipose-specific *Raptor* knockout, result in lean mice with increased energy expenditure (Polak et al., 2008). However, some studies show an absence of changes in BW or even an increase with rapamycin treatment in mice (Fischer et al., 2015; Liu et al., 2014; Zhang et al., 2013b). Thus, the link between mTOR signaling, the effects of rapamycin, and fat metabolism remains unresolved (Cai et al., 2016).

Compared with the numerous studies on mTORC1, knowledge of the role of mTORC2 in metabolism is less understood (Albert and Hall, 2015) and is confounded by the multi-level crosstalk between the two complexes (Julien et al., 2010). Unlike mTORC1, mTORC2 is largely insensitive to rapamycin in an acute setting; however, it can be inhibited by chronic exposure to rapamycin in vitro (Sarbassov et al., 2006). Chronic rapamycin treatment also disrupted both mTORC1 and mTORC2 complexes in muscle, liver, and adipose tissues (Lamming et al., 2012; Schreiber et al., 2015). Interestingly, inactivation of mTORC2 signaling by deletion of *Rictor* specifically in adipose tissue of mice also profoundly affects whole-body metabolism, leading to weight gain and insulin resistance (Kumar et al., 2010) and suggesting that whole-body metabolism could be affected only by altered mTORC2 activity in adipose tissues.

Over 450 distinct mutations in *LMNA* that encode A-type lamins that form intermediate filaments in the nucleus cause a range of diseases termed laminopathies (Schreiber and Kennedy, 2013). The laminopathies comprise multiple diseases with a range of phenotypic overlap (Worman and Bonne, 2007), including different forms of cardiomyopathy, muscular dystrophy, lipodystrophy, neuropathy, and progeria (Hutchinson-Gilford progeria syndromes, HGPSs). Lamin A/C-deficient (*Lmna*$^{-/-}$) mice, which are really hypomorphs because of low-level expression of an altered splice variant (Jahn et al., 2012), can capture some of those phenotypes, including cardiomyopathy, muscular dystrophy, neuropathy, and, possibly, lipodystrophy (Sullivan et al., 1999). Previously, we found that dilated cardiomyopathy and skeletal muscle dystrophy is associated with aberrantly elevated mTORC1 signaling (Ramos et al., 2012), a result consistent with findings in mice expressing a *Lmna* variant, H222P, associated with

cardiomyopathy (Choi et al., 2012). Rapamycin-mediated mTORC1 inhibition improves cardiac and muscle function and robustly enhances survival in *Lmna*$^{-/-}$ mice (Ramos et al., 2012). Given the role of mTOR activity in regulating cellular metabolism, we speculated that aberrant mTOR signaling may be fundamental to the development of lipodystrophy in *Lmna*$^{-/-}$ mice and, possibly, human patients, as well. Here we examined whether life extension by rapamycin in *Lmna*$^{-/-}$ mice is due to the mTOR-mediated regulation of lipid metabolism in adipose tissue.

RESULTS

Rapamycin Increases Body Weight and Fat Content in the Context of *Lmna*$^{-/-}$ Mice

Previously, we reported that the survival of *Lmna*$^{-/-}$ mice can be extended by rapamycin (Ramos et al., 2012). To examine metabolic phenotypes and the consequences of rapamycin administration in more detail, we repeated this experiment, delivering rapamycin by intraperitoneal injection every other day. The results validate the previous findings, indicating that *Lmna*$^{-/-}$ mice treated with rapamycin lived approximately twice as long as control littermates (Figure 1A; Figure S1).

Lmna$^{-/-}$ mice rapidly become cachexic, losing BW significantly before death. Interestingly, and consistent with enhanced survival, the drug partially suppressed the rapid weight loss in *Lmna*$^{-/-}$ mice (Figure 1B). However, rapamycin-treated *Lmna*$^{-/-}$ mice still undergo a significant weight decline before death, suggesting that cachexia may still contribute to their mortality. Consistent with BW data, rapamycin-treated *Lmna*$^{-/-}$ mice showed a significant increase in total fat content (Figure 1C). These findings suggested that, in addition to the potential direct benefits of rapamycin on cardiac and muscle function (Ramos et al., 2012), increasing fat content may be a factor in the improved survival of *Lmna*$^{-/-}$ mice. Interestingly, this short-term treatment with rapamycin does not increase the BW of wild-type (WT) mice but tends to increase the percentage of fat (Figures S1G and S1H).

Rapamycin Suppresses Elevated Energy Expenditure in *Lmna*$^{-/-}$ Mice

Energy balance is determined by energy intake and expenditure. We then employed indirect calorimetry to characterize the metabolic profiles of *Lmna*$^{-/-}$ mice treated with rapamycin to decipher the cause(s) of the lean phenotype. Interestingly, *Lmna*$^{-/-}$ mice exhibit high energy expenditure (EE) both during the day and night cycle (Figure 1D). Consistent with our hypothesis, rapamycin completely reversed this elevated EE (Figure 1D). Paradoxically, but perhaps consistent with their muscle pathology, *Lmna*$^{-/-}$ mice were hypoactive relative to controls, as shown by decreased movement in wheel running and pedestrian walking (Figure S2). Thus, we excluded the possibility of a significant increase in behavioral activity that contributes to the elevated EE in *Lmna*$^{-/-}$ mice (Figure S2). As reported, *Lmna*$^{-/-}$ mice eat substantially less even when food intake is adjusted to BW (Nikolova et al., 2004; Figure 1F). However, we were unable to detect any significant increase in food intake in rapamycin-treated *Lmna*$^{-/-}$ mice (Figure 1F), indicating that other differences likely account for the altered fat content in these mice. In summary, we found that reduced fat depots in *Lmna*$^{-/-}$ mice resulted from reduced energy intake and elevated EE and that rapamycin suppressed this elevated EE to a level comparable with WT mice (Figure 1D). This suppression of elevated EE suggested that the metabolic effects of rapamycin may in part underlie the health benefits of the drug in *Lmna*$^{-/-}$ mice.

To estimate fuel utilization, we measured the respiratory quotient (RQ) in the same setting. *Lmna*$^{-/-}$ mice have indistinguishable fuel utilization compared with WT mice either during the day or night cycle (Figure 1E), suggesting that the loss in fat in *Lmna*$^{-/-}$ mice is not a result of altered substrate utilization for energy production. However, the rapamycin-treated *Lmna*$^{-/-}$ mice had a significantly decreased RQ compared with their *Lmna*$^{-/-}$ controls during the day cycle and exhibited a similar (although not significant) trend at night (Figure 1E), suggesting that rapamycin enhanced fat utilization in *Lmna*$^{-/-}$ mice even while simultaneously maintaining fat content. We consistently observed no difference in RQ in WT mice treated with rapamycin, as reported previously (Fang et al., 2013).

Collectively, the data suggest that the lean phenotype of *Lmna*$^{-/-}$ mice is likely due to increased EE rather than changes caused by energy intake or activity. Also, rapamycin promotes weight gain in *Lmna*$^{-/-}$ mice by suppressing EE rather than increasing food intake or decreasing behavioral activity.

Rapamycin Suppresses Elevated Lipolysis in White Adipose Tissue of *Lmna*$^{-/-}$ Mice

Activation of mTOR signaling promotes adipogenesis and suppresses lipogenesis in WT mice (Lamming and Sabatini, 2013). In addition, we have demonstrated that mTORC1 signaling is elevated in the heart and skeletal muscle of *Lmna*$^{-/-}$ mice (Ramos et al., 2012). Therefore, we speculated that the dysregulation of mTOR signaling might contribute to the lipodystrophy in *Lmna*$^{-/-}$ mice. To test this, we characterized mTOR signaling in adipose tissue of *Lmna*$^{-/-}$ mice and its regulation by rapamycin. In the white adipose tissue (WAT) of *Lmna*$^{-/-}$ mice, mTORC1 activity, as indicated by phosphorylation of rpS6 (p-S6 S240/244), was not statistically different from that of WT mice (Figure 2A), suggesting that WAT may not be the major pathological tissue accounting for the short lifespan of *Lmna*$^{-/-}$ mice. Because mTORC1 signaling is also not increased in the liver of *Lmna*$^{-/-}$ mice (Ramos et al., 2012), this finding further supports the observation that elevated mTORC1 signaling in *Lmna*$^{-/-}$ mice is a tissue-specific phenomenon. We also determined mTORC2 activity indicated by p-Akt (S473), p-SGK (S422), and p-NDRG1 (T346). We found that mTORC2 activity is increased in *Lmna*$^{-/-}$ mice, although we also found no significant change in p-Akt (S473) (Figure 2D) but a significant change in p-SGK (S422) and p-NDRG1 (T346) (Figure S3A).

As with the heart and skeletal muscle of *Lmna*$^{-/-}$ mice (Ramos et al., 2012), rapamycin strongly suppressed mTORC1 signaling in WAT (Figure 2B), mirroring findings in WT mice (Figure 2C). Chronic rapamycin treatment has been shown to disrupt mTORC2 and thus suppress p-Akt in adipose tissue of WT mice (C57BL/6J) (Lamming et al., 2012; Schreiber et al., 2015) and in our colony (mixed 129Sv-C57BL/6J) (Figure 2F). However,

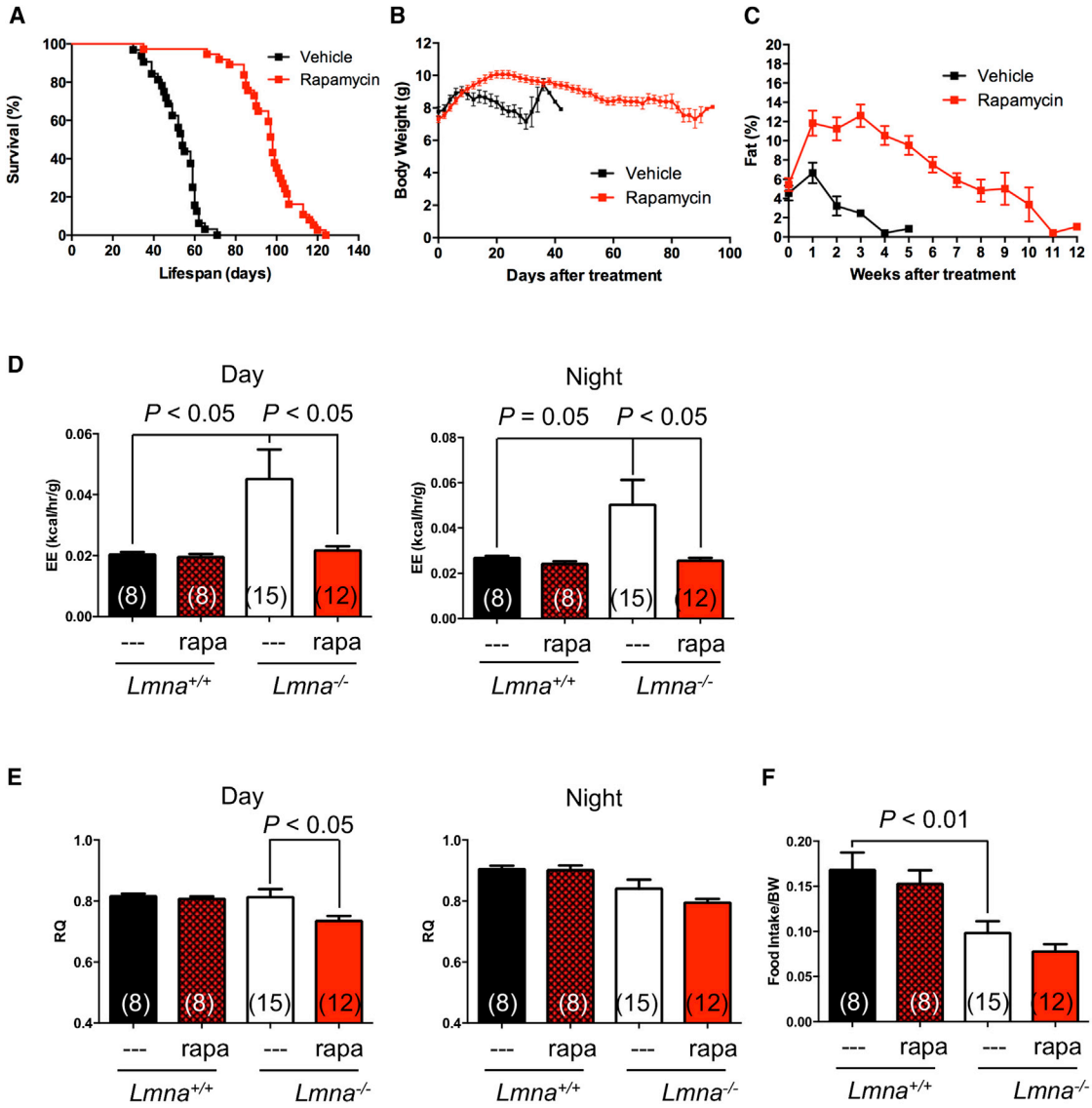

Figure 1. Lamin A/C-Deficient Mice Treated with Rapamycin Live Longer and Maintain More Body Weight and Adiposity

(A) Kaplan-Meier plot of *Lmna*$^{-/-}$ mice that were treated with vehicle (n = 32, black) or rapamycin (n = 37, red) every other day starting at 4 weeks of age. Symbols represent individual mice.

(B) *Lmna*$^{-/-}$ mice treated with vehicle (n = 32, black) or rapamycin (n = 38, red) were weighed every other day.

(C) Adiposity (percent body fat) was measured weekly ([fat mass/BW] × 100) from mice treated with vehicle (n = 8, black) or rapamycin (n = 11, red). Symbols represent mean BW or percent body fat ± SEM.

(D and E) EE (D) and RQ (E) of *Lmna*$^{+/+}$ and *Lmna*$^{-/-}$ mice treated with rapamycin (rapa) during the day and night cycle.

(F) Food intake of *Lmna*$^{+/+}$ and *Lmna*$^{-/-}$ mice treated with rapa. Data from males and females are combined.

Each value is mean ± SEM for the number of mice indicated in parentheses.

we failed to detect a reduction in p-Akt (S473) by rapamycin in WAT of *Lmna*$^{-/-}$ mice (Figure 2E). The same pattern is seen for other substrates of mTORC2, p-SGK (S422) and p-NDRG1 (T346) (Figure S3B). Thus, although mTORC1 signaling is not intrinsically altered in WAT of *Lmna*$^{-/-}$ mice, altered fat storage by rapamycin in *Lmna*$^{-/-}$ mice may be related to the suppression of mTORC1 activity but not mTORC2.

Next we examined proteins involved in lipid metabolism to look for other molecular explanations underlying the decreased adiposity of *Lmna*$^{-/-}$ mice. We found that the reduction in adiposity in *Lmna*$^{-/-}$ mice is not linked to altered expression of proteins involved in lipogenesis, such as fatty acid synthase (FAS) (Figure S3E). Furthermore, although rapamycin-treated *Lmna*$^{-/-}$ mice maintained more adiposity, this is also unlikely to be due to enhanced lipogenesis (Figure S3F). Of note, rapamycin did suppress FAS in WT mice (Figure S3G).

For lipolysis, adipose triglyceride lipase (ATGL) and hormone-sensitive lipase (HSL) are responsible for most of the

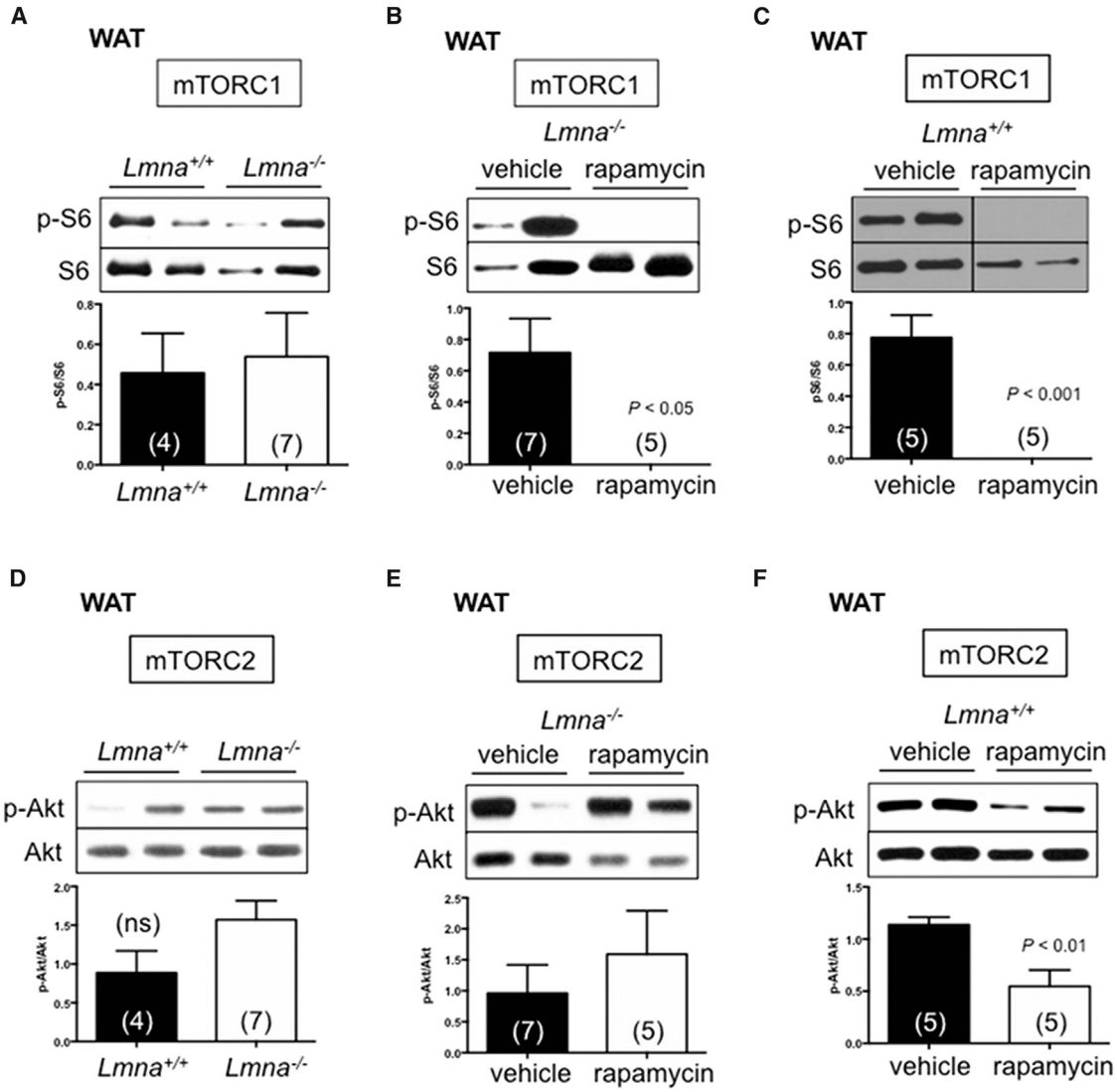

Figure 2. Role of mTOR Activity in White Adipose Tissue of *Lmna*$^{+/+}$ and *Lmna*$^{-/-}$ Mice Treated with Rapamycin

(A–C) Western blots of mTORC1 activity in WAT of *Lmna*$^{+/+}$ and *Lmna*$^{-/-}$ mice treated with rapamycin. Relative p-S6 levels (normalized to S6) were quantified. (D–F) Western blots of mTORC2 activity in WAT of *Lmna*$^{+/+}$ and *Lmna*$^{-/-}$ mice treated with rapamycin. Relative p-Akt levels (normalized to Akt) were quantified. Each value is mean ± SEM for the number of mice indicated in parentheses. p values were derived from unpaired two-tailed Student's t test. ns, no significance.

triglyceride hydrolase activity in murine WAT (Schweiger et al., 2006; Figure 3A). Consistent with our hypothesis, ATGL was elevated in *Lmna*$^{-/-}$ mice, suggesting increased breakdown of fat reserves in WAT (Figure 3B) as well as the elevation of serum free fatty acids (FFAs) (Figure 3H), a lipolysis product. Interestingly, rapamycin suppressed this effect (Figures 3C and 3H). In contrast, p-HSL (S563) was not affected by loss of A-type lamins or rapamycin (Figures 3E and 3F). Of note, rapamycin did not significantly suppress lipolysis in WT mice (Figures 3D and 3G).

We further tested this rapamycin-suppressed lipolysis in adipocytes purified from adipose tissue. We found that rapamycin suppressed ATGL levels after 24 hr of treatment in preadipocyte cells derived from WAT of *Lmna*$^{-/-}$ mice (Figure 3I). Together, these data indicate that the disappearance of fat in *Lmna*$^{-/-}$ mice is associated with increased lipolysis in WAT and that this phenotype is suppressed by rapamycin.

Altered UCP1 Expression in Brown Adipose Tissue of *Lmna*$^{-/-}$ Mice

We considered the likelihood that increased EE and reduced adiposity in *Lmna*$^{-/-}$ mice may be due to altered mitochondrial uncoupling and heat generation mediated by uncoupling protein 1 (UCP1) in brown adipose tissue (BAT). Interestingly, both mTORC1 and mTORC2 signaling have been thought to suppress UCP1 expression in WT mice, although the molecular mechanisms are not well established (Cai et al., 2016; Figure 4A).

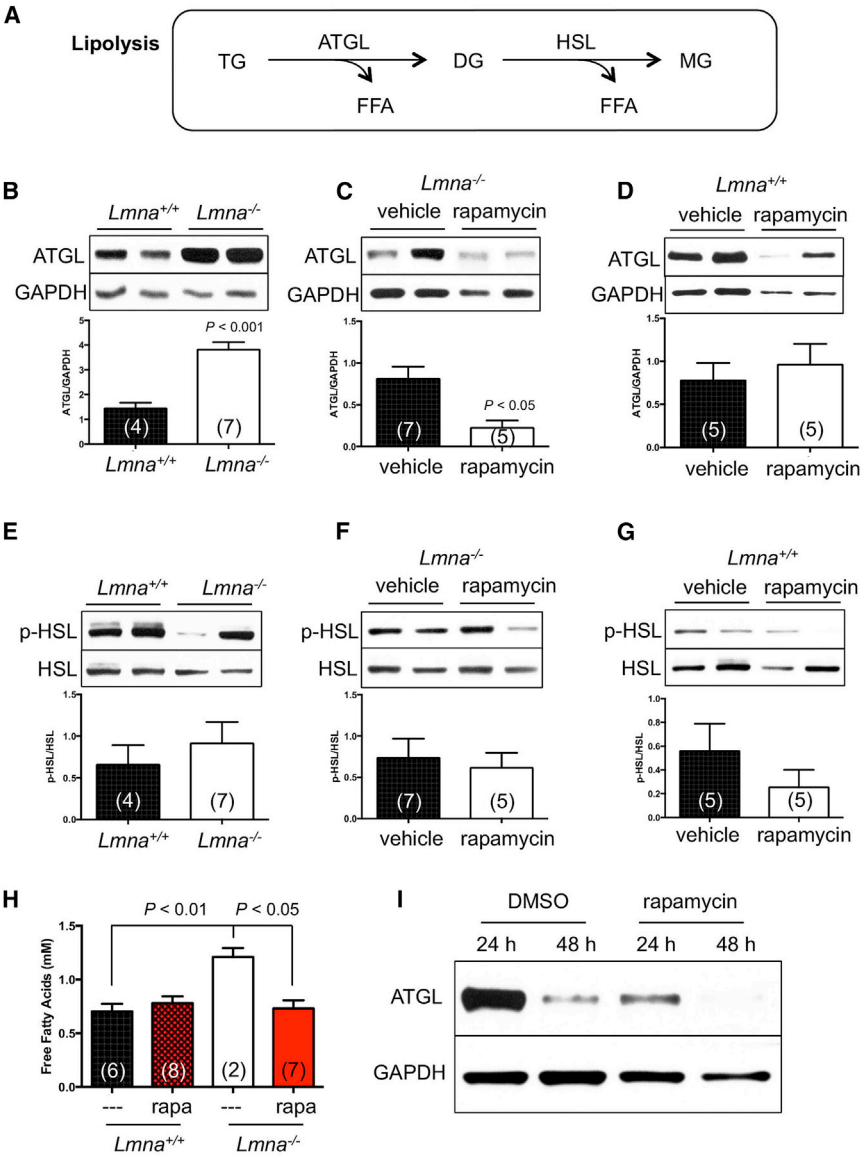

Figure 3. Rapamycin Reverses the Elevated Lipolysis in White Adipose Tissue of *Lmna*$^{-/-}$ Mice

(A) Simplified diagram of the lipolytic pathway in WAT. TG, triglyceride; DG, diglyceride; MG, monoacylglycerol.

(B–D) Activity of lipolysis, indicated by ATGL, of *Lmna*$^{+/+}$ and *Lmna*$^{-/-}$ mice treated with rapamycin. Relative ATGL levels (normalized to GAPDH) were quantified.

(E–G) Activity of lipolysis, indicated by p-HSL, of *Lmna*$^{+/+}$ and *Lmna*$^{-/-}$ mice treated with rapamycin. Relative p-HSL levels (normalized to HSL) were quantified.

(H) FFA of *Lmna*$^{+/+}$ and *Lmna*$^{-/-}$ mice treated with rapamycin.

(I) Western blots of ATGL levels in preadipocytes derived from WAT of *Lmna*$^{-/-}$ mice. Representative blots from five *Lmna*$^{-/-}$ mice are shown.

Each value is mean ± SEM for the number of mice indicated in parentheses. p values were derived from unpaired two-tailed Student's t test.

In light of the role of BAT in mammalian physiology, we also examined mTOR signaling in BAT. Interestingly, we observed elevation of mTORC1 signaling in BAT of *Lmna*$^{-/-}$ mice, as indicated by p-S6 (Figure 4B). The same pattern is seen for the activity of mTORC2 signaling, as indicated by p-Akt (S473) (Figure 4E). Phosphorylation of NDRG1 (T346) may also be elevated, although the difference did not reach significance, and no changes were observed for p-SGK (S422) (Figure S3C). This suggests that aberrant mTOR signaling in BAT may contribute to the elevated EE in *Lmna*$^{-/-}$ mice, especially mTORC1 signaling. Rapamycin suppressed mTORC1 (Figure 4F) but not mTORC2, as indicated by p-Akt (S473) (Figure 4F) and p-SGK (S422) (Figure S3D) in BAT of *Lmna*$^{-/-}$ mice. Suppression of p-S6 but not p-Akt (S473) was also found in WT mice (Figures 4D and 4G).

Consistent with previous reports (Xiang et al., 2015; Figure 4A), we detected a downregulation of UCP1 in BAT of *Lmna*$^{-/-}$ mice concomitant with elevated mTOR activity (Figure 4H). This suggests that *Lmna*$^{-/-}$ mice suffer from a mis-regulation of thermogenesis. Interestingly, rapamycin restored UCP1 expression in BAT (Figure 4I), suggesting enhanced thermogenesis coupled with reduced EE. Consistent with these results, we found that the body temperature was better maintained in rapamycin-treated *Lmna*$^{-/-}$ mice, a mouse model with intrinsic hypothermia (Figure 4K). To confirm that rapamycin directly mediates UCP1 expression in BAT, we isolated BAT from *Lmna*$^{-/-}$ mice and cultured preadipocytes that were treated with or without rapamycin. We found that the UCP1 level was indeed elevated by rapamycin in this setting (Figure 4L). Together, these data imply that rapamycin enhances heat production in *Lmna*$^{-/-}$ mice, either through direct regulation of UCP1 or indirectly as a result of suppression of EE through other mechanisms.

Higher Housing Temperature Suppresses Energy Expenditure and Extends Survival of *Lmna*$^{-/-}$ Mice

Given their smaller size, elevated EE, and reduced expression of UCP1 in BAT of *Lmna*$^{-/-}$ mice, we tested the hypothesis that increasing ambient temperature would suppress EE and enhance the survival of *Lmna*$^{-/-}$ mice. As predicted, an ambient temperature of 30°C, which represents thermoneutrality, dramatically suppressed elevated EE in *Lmna*$^{-/-}$ mice (Figure S4A). However, fuel utilization was not altered because the RQ was indistinguishable from *Lmna*$^{-/-}$ mice at 22°C (Figure S4B), indicating that *Lmna*$^{-/-}$ mice at 30°C do not switch to fat as a major energy source.

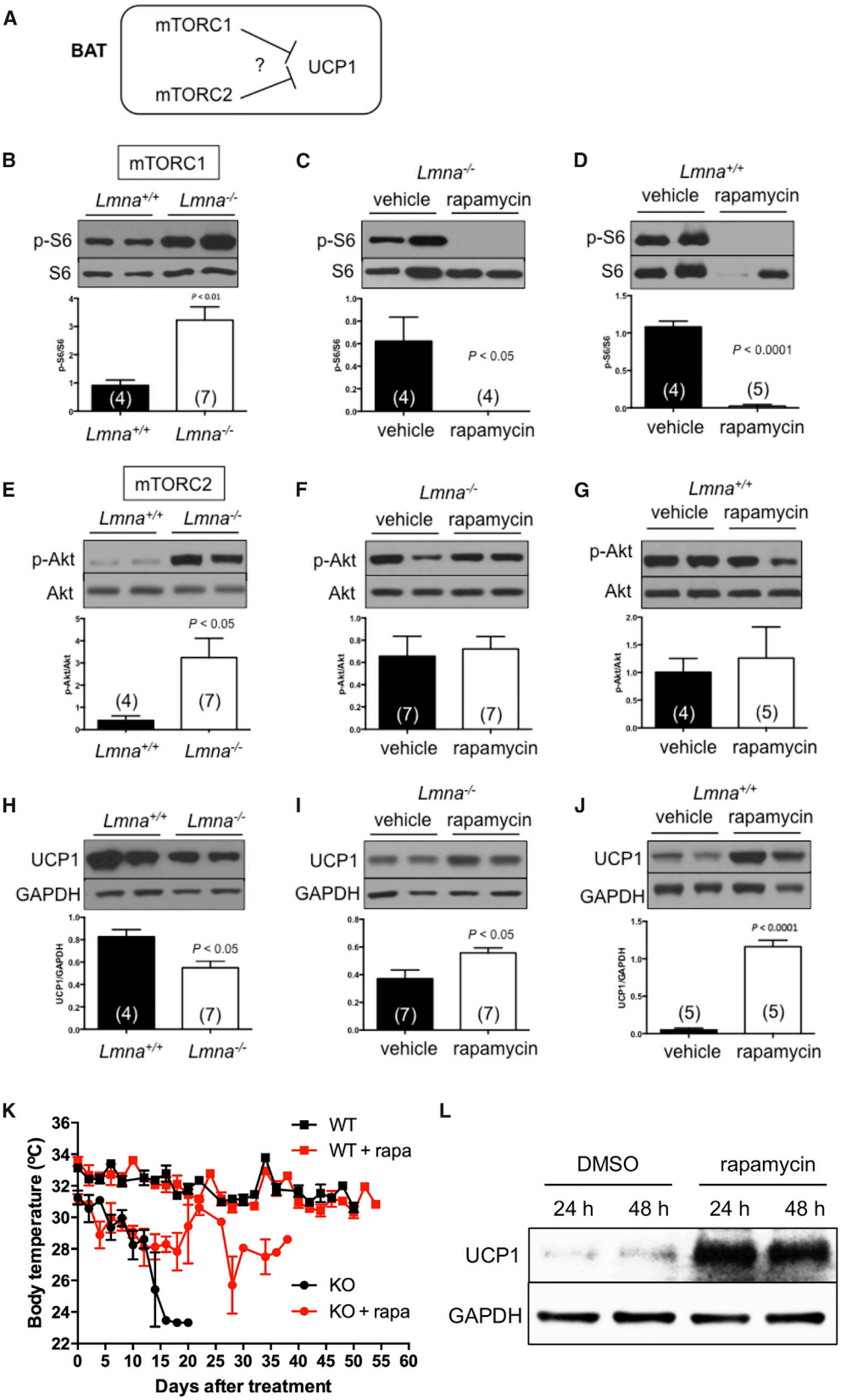

(legend on next page)

A higher housing temperature also extended the survival of *Lmna*$^{-/-}$ mice (Figure 5A; Figures S4D and S4G). *Lmna*$^{-/-}$ mice housed under 30°C also gained more BW and body fat than control mice (Figures 5B and 5C; Figures S4E, S4F, S4H, and S4I). Surprisingly, *Lmna*$^{-/-}$ mice under 30°C ate less than *Lmna*$^{-/-}$ mice at 22°C (Figure S4C).

At the molecular level, 30°C suppressed lipolysis in WAT (Figure 5D), which may contribute to maintaining more BW and adiposity in *Lmna*$^{-/-}$ mice (Figures 5B and 5C). Also, UCP1 protein in BAT was suppressed by 30°C (Figure 5H), which is also consistent given the reduced need for thermogenesis. Together, these findings indicate that thermoneutral conditions are sufficient to extend the lifespan of *Lmna*$^{-/-}$ mice. Of note, however, the enhancement of survival by 30°C is less than that caused by rapamycin even though suppression of EE is more robust at 30°C, indicating that the magnitudes of the two phenotypes are not directly correlated.

Notably, elevated EE was not observed in *Lmna*$^{H222P/H222P}$ mice, which model a human mutation associated with dilated cardiomyopathy and muscular dystrophy without lipodystrophy (Arimura et al., 2005). As with the *Lmna*$^{-/-}$ mice (Ramos et al., 2012), suppressing mTORC1 signaling ameliorates cardiomyopathy in *Lmna*$^{H222P/H222P}$ mice (Choi et al., 2012); however, unlike the *Lmna*$^{-/-}$ mice, it does not extend the lifespan (Figure S5).

Collectively, we interpret our data to mean that reduced EE accounts for a portion of the survival benefits conferred by rapamycin but not all. This implies that rapamycin enhances survival in *Lmna*$^{-/-}$ mice either through improvements in cardiac or skeletal muscle function, even though this was insufficient to affect survival in *Lmna*$^{H222P/H222P}$ mice, or through other unknown physiologic consequences, perhaps related to aspects of metabolism not phenocopied by thermoneutrality.

DISCUSSION

Lmna$^{-/-}$ mice, used commonly as a model for the cardiomyopathy and muscular dystrophy associated with human mutations in *LMNA* (Schreiber and Kennedy, 2013; Zhang et al., 2013a), are also reported to be lean (Sullivan et al., 1999), and this has been speculated to be a consequence of their myopathic disease rather than lipodystrophy (Cutler et al., 2002). Here we show that *Lmna*$^{-/-}$ mice have elevated EE. Furthermore, we demonstrate that both rapamycin and 30°C suppress EE, slow down BW and body fat loss, and significantly extend survival. Molecularly, the pronounced high EE developed in *Lmna*$^{-/-}$ mice can be attributed in part to the downregulation of thermogenic protein UCP1 expression in BAT, which leads to an increase of lipolysis in WAT to provide FFAs as energy to compensate. All of these phenotypes can be rescued by rapamycin, which suppressed the elevated mTORC1 activity in the BAT of *Lmna*$^{-/-}$ mice (Figure 5I). This model could be supported by UCP1-deficient mice, which show a great loss of BW and fat mass consistent with increased EE (Ukropec et al., 2006), and ATGL knockout mice, which accumulate fat mass with reduced EE (Haemmerle et al., 2006).

In addition to the cardiac and skeletal muscle phenotypes, *Lmna*$^{-/-}$ mice present with a lipodystrophic phenotype that appears to be similar to that recently observed in HGPS model *Lmna*$^{G609G/G609G}$ mice, including increased WAT lipolysis and elevated EE (Lopez-Mejia et al., 2014). The HGPS mutation that leads to progerin expression is complex in nature, likely evoking both gain-of-function and loss-of-function phenotypes. We speculate that the lipodystrophic phenotype may be loss of function, an assertion supported by the existence of human lipodystrophic mutations that act recessively.

Multiple mouse models of HGPS, including *Zmpste24*$^{-/-}$ (defective for prelamin A processing) and the aforementioned *Lmna*$^{G609G/G609G}$, show a loss of adiposity. Proteomic profiling of adipose tissue from *Zmpste24*$^{-/-}$ mice showed upregulation of ATGL (Peinado et al., 2011) consistent with increased lipolysis. Moreover, interventions associated with enhanced survival in these models also lead to delayed weight loss and/or increased fat content. These include *Zmpste24*$^{-/-}$ mice treated with resveratrol (Liu et al., 2012), recombinant IGF-1 (Mariño et al., 2010), and the farnesyltransferase inhibitor (Fong et al., 2006) as well as *Lmna*$^{G609G/G609G}$ mice exposed to an antisense morpholino treatment strategy designed to block the pathogenic *Lmna* splicing that leads to progerin expression (Osorio et al., 2011). We speculate that a higher housing temperature may improve survival in these mouse models and propose that restoration of adipose tissue may be critical to therapeutic approaches in HGPS patients as well as those with lipodystrophy.

Regarding mTOR signaling, the most striking observation in this study is that rapamycin-treated *Lmna*$^{-/-}$ mice maintained more BW, which is due to an increase in fat content. This adds to increasing evidence suggesting that mTOR signaling plays a role in lipid homeostasis and that mTORC1 exerts a positive role in adipogenesis (Chakrabarti et al., 2010; Lamming and Sabatini, 2013). We observed elevated lipolysis in *Lmna*$^{-/-}$ mice, indicated by enhanced ATGL expression and increased serum FFAs. This phenotype was not associated with altered mTOR signaling in WAT, but rapamycin strongly suppressed it, consistent with observations in other contexts that rapamycin can suppress ATGL expression (Chakrabarti et al., 2010, 2013).

Figure 4. Rapamycin Reverses the Downregulated UCP1 Protein in Brown Adipose Tissue of *Lmna*$^{-/-}$ Mice

(A) Tested model for the role of mTOR activity in the expression of UCP1 protein in BAT.

(B–D) Western blots of mTORC1 activity in *Lmna*$^{+/+}$ and *Lmna*$^{-/-}$ mice treated with rapamycin. Relative p-S6 levels (normalized to S6) were quantified.

(E–G) Western blots of mTORC2 activity of *Lmna*$^{+/+}$ and *Lmna*$^{-/-}$ mice treated with rapamycin. Relative p-Akt levels (normalized to Akt) were quantified.

(H–J) Rapamycin increases UCP1 in BAT of *Lmna*$^{-/-}$ mice. Relative UCP1 levels (normalized to GAPDH) were quantified.

(K) Body surface temperature of *Lmna*$^{+/+}$ and *Lmna*$^{-/-}$ mice treated with rapamycin. Mice treated with vehicle (WT, black square, n = 4; knockout [KO], black circle, n = 11) or rapamycin (WT, red square, n = 5; KO, red circle, n = 11) were measured every other day. Symbols represent mean body surface temperature ± SEM. Data from males and females are combined.

(L) Western blots of UCP1 levels in preadipocytes derived from BAT of *Lmna*$^{-/-}$ mice. Representative blots from five *Lmna*$^{-/-}$ mice are shown.

Each value is mean ± SEM for the number of mice indicated in parentheses. p values were derived from unpaired two-tailed Student's t test.

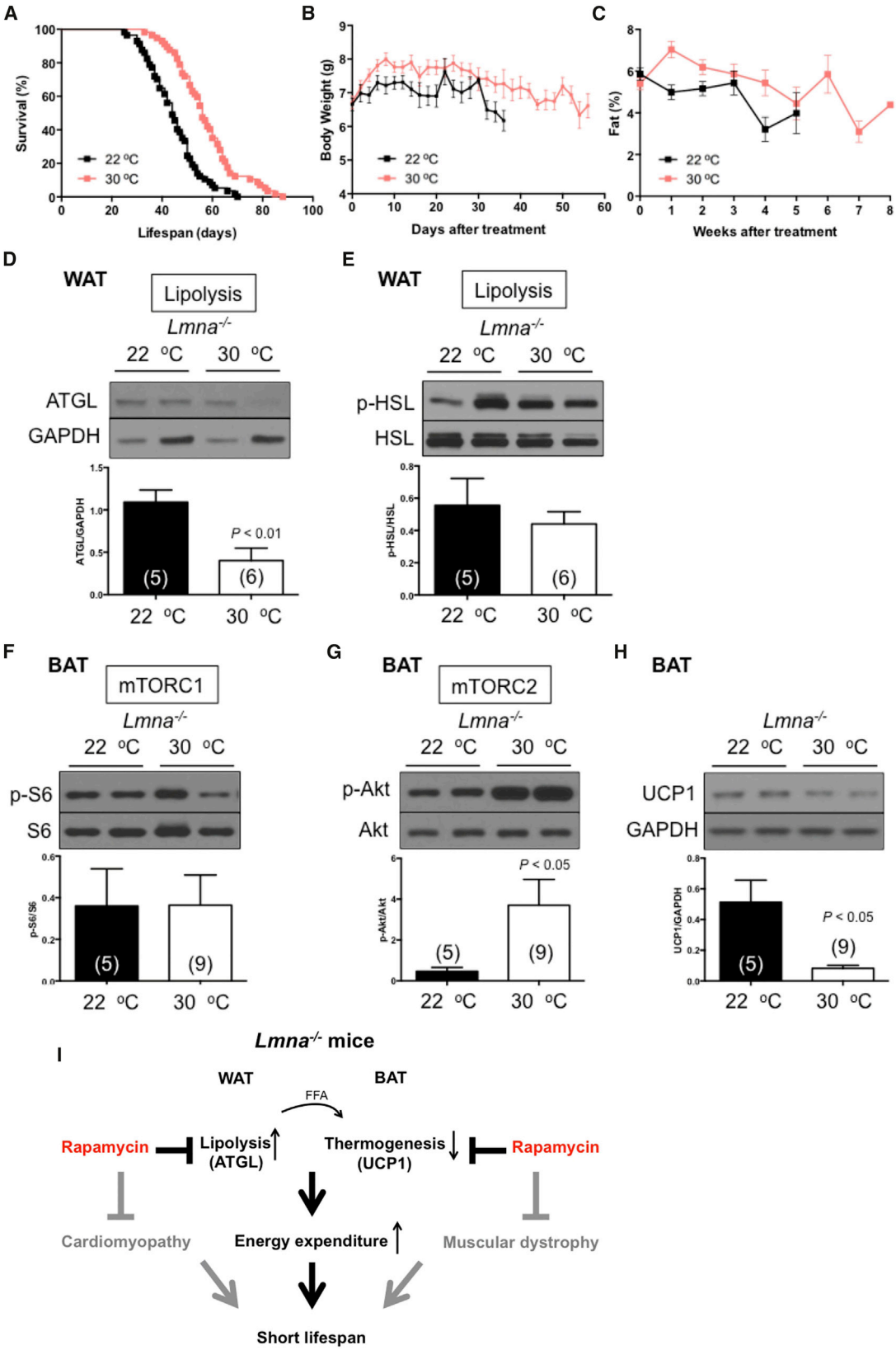

(legend on next page)

Contrary to WAT, both mTORC1 and mTORC2 signaling are elevated in BAT, implying a link between A-type lamin function and mTOR signaling in BAT and suggesting that metabolic dysregulation in *Lmna*$^{-/-}$ mice may be related to altered BAT function. Consistently, we found that the thermogenic protein UCP1 was downregulated in BAT of *Lmna*$^{-/-}$ mice and restored by rapamycin. Given that UCP1 functions as a H^+/fatty acid symporter, fatty acids produced from lipolysis of WAT were revealed to allosterically activate UCP1-mediated uncoupling (Fedorenko et al., 2012). Thus, the working model is that rapamycin suppresses elevated EE in *Lmna*$^{-/-}$ mice in part by restoring UCP1 protein level in BAT, which leads to efficient use of the FFA from lipolysis of WAT as an energy resource. Further, rapamycin suppresses lipolysis in WAT, which contributes to increased BW and adiposity as well as suppression of elevated EE in *Lmna*$^{-/-}$ mice (Figure 5I). In addition, the elevated mTORC1 signaling in BAT may in part account for the reduced UCP-1-mediated uncoupling and impaired thermogenic function observed in mTORC1-hyperactive animal models such as *Lmna*$^{-/-}$ mice. Interestingly, and as opposed to rapamycin, UCP1 levels in BAT were further suppressed by 30°C in *Lmna*$^{-/-}$ mice, and mTORC2 activity was further increased (Figure 5). The reasons for this are unclear.

Collectively, this study provides insight into how high EE may contribute to lipodystrophy and how approaches that can suppress EE, such as rapamycin and higher housing temperature, can prolong survival of *Lmna*$^{-/-}$ mice. Our findings show that maintaining more adiposity may be an affective therapeutic approach in a subset of laminopathies, including progeroid syndromes. These findings, coupled with our previous report (Ramos et al., 2012), also further demonstrate the potential utility of rapamycin and related rapalogs in treatment of a range of laminopathies.

EXPERIMENTAL PROCEDURES

Mouse Husbandry

Lmna$^{+/-}$ mice (129Sv-C57BL/6J genetic background) were crossed to generate *Lmna*$^{+/+}$ and *Lmna*$^{-/-}$ mice (Sullivan et al., 1999). Three-week-old littermate mice from *Lmna*$^{+/-}$ x *Lmna*$^{+/-}$ crosses were weaned and genotyped. *Lmna*$^{H222P/+}$ mice were crossed to generate *Lmna*$^{+/+}$ and *Lmna*$^{H222P/H222P}$ mice (129SvJ-C57BL/6J genetic background) as described in a previous study (Arimura et al., 2005). All animals had food and water ad libitum and were kept at 22°C and 12:12-h light/dark cycles. All animal care and experimental procedures were approved by the Institutional Animal Care and Use Committee (IACUC) at the Buck Institute for Research on Aging.

Lifespan Study on Rapamycin Injection

Beginning at 4 weeks of age, mice were injected intraperitoneally with 8 mg/kg BW rapamycin (LC Laboratories) or vehicle every other day and maintained for the remainder of their lifespan according to the protocol by Ramos et al. (2012). Briefly, a stock solution of rapamycin (50 mg/ml) was prepared in 100% ethanol and stored at −20°C. Rapamycin was then diluted in vehicle (5% polyethylene glycol and 5% Tween 80) before injection. The vehicle control consisted of the same volume of ethanol.

Lifespan Study on 30°C Ambient Temperature

Mice were randomly chosen to be housed at 22°C or 30°C starting at 4 weeks of age and maintained at these temperatures until the *Lmna*$^{-/-}$ mice reached the end of their lives.

Lifespan Study on Rapamycin Chow

After genotyping, 2-month-old *Lmna*$^{H222P/H222P}$ mice were treated with a micro-encapsulated rapamycin diet (14 ppm) or control diet fed ad libitum (Harrison et al., 2009) until they died.

Body Composition

Whole-body composition analysis was conducted weekly using a quantitative nuclear magnetic resonance machine (EchoMRI-2012, Echo Medical Systems).

Indirect Calorimetry

Metabolism was measured in a Promethion metabolic cage system (Sable Systems International) equipped with GA-3 small mammal gas analyzers. Metabolic cages were used while the mice were awake to simultaneously measure BW, EE, physical activity, and food intake. Four-week-old mice injected for 2 weeks with rapamycin were subjected to recording. Mice were housed individually in metabolic cages and acclimatized for 24 hr before the beginning of the recording and the analysis. Conditions were the same for the 30°C study except for the temperature in the metabolic cages. Data were subsequently analyzed using Sable System ExpeDATA software (v1.4.9).

Free Fatty Acid

Mice were fasted 16 hr after 2 weeks of treatment for submandibular bleeding. Serum was separated by centrifugation at 4°C and stored at −80°C. Free fatty acid (Wako Diagnostics, Mountain View, CA) was determined by following the manufacturer's instructions.

Body Surface Temperature

Body surface temperature was measured with an infrared temperature probe (Infrascan, La Crosse Technology) directed at the abdomen of all single-housed mice.

Tissue Harvesting and Immunoblotting

After 2 weeks of treatment, subcutaneous fat (WAT) and BAT were harvested and immediately frozen in liquid nitrogen for western blotting analysis. Tissues were homogenized using the Omni TH homogenizer (Omni International) on ice in Radioimmunoprecipitation assay (RIPA) buffer (300 mM NaCl, 1.0% NP-40, 0.5% sodium deoxycholate, 0.1% SDS, 50 mM Tris [pH 8.0], protease inhibitor

Figure 5. Higher Housing Temperature Increases Survival in *Lmna*$^{-/-}$ Mice

(A) Kaplan-Meier plot of *Lmna*$^{-/-}$ mice that were treated at 22°C (n = 57, black) or 30°C (n = 57, pink). Symbols represent individual mice. Data from males and females are combined.

(B) Mice treated at 22°C (n = 57, black) or 30°C (n = 56, pink) were weighed every other day.

(C) Adiposity (percent body fat) was measured weekly ([fat mass/BW] × 100) from mice treated at 22°C (n = 58, black) or 30°C (n = 55, pink). Symbols represent mean BW or percent body fat ± SEM.

(D and E) Lipolysis in WAT of *Lmna*$^{-/-}$ mice treated at 22°C or 30°C. Relative ATGL levels (normalized to GAPDH) and p-HSL levels (normalized to HSL) were quantified.

(F) Western blots of mTORC1 activity in BAT of *Lmna*$^{-/-}$ mice at 30°C. Relative p-S6 levels (normalized to S6) were quantified.

(G) Western blots of mTORC2 activity in BAT of *Lmna*$^{-/-}$ mice at 30°C. Relative p-Akt levels (normalized to Akt) were quantified.

(H) UCP1 protein expression was suppressed by 30°C in BAT of *Lmna*$^{-/-}$ mice.

(I) Schematic explaining the functional role of rapamycin in WAT and BAT in life extension of *Lmna*$^{-/-}$ mice. See Discussion for details.

Each value is mean ± SEM for the number of mice indicated in parentheses. p values were derived from unpaired two-tailed Student's t test.

cocktail [Roche], and phosphatase inhibitor 2, 3 [Sigma]) and then centrifuged at 13,200 rpm for 10 min at 4°C. The supernatants were collected, and protein concentrations were determined using the detergent compatible (DC) protein assay (Bio-Rad). Equal amounts of protein were resolved by SDS-PAGE (4%–12% Bis-Tris gradient gel, Invitrogen), transferred to membranes, and incubated with protein-specific antibodies. The antibodies against phosphorylated rsS6$^{S240/244}$ (5364), Akt^{S473} (4058), NDRG1^{T346} (5482), HSL^{S563} (4139), S6 (2217), Akt (4691), ATGL (2439), HSL (4107), FAS (3180), and glyceraldehyde 3-phosphate dehydrogenase (GAPDH; 2118) were purchased from Cell Signaling Technology. The antibodies against phosphorylated SGK^{S422} (16745R) and NDRG1 (398291) were purchased from Santa Cruz Biotechnology. SGK (54726) was purchased from GeneTex. UCP1 (ab23841) was purchased from Abcam. Protein bands were revealed using the Amersham enhanced chemiluminescence (ECL) detection system (GE Healthcare) and quantified by densitometry using ImageJ software (http://rsb.info.nih.gov/ij/).

Isolation and Culture of Preadipocytes

Mouse primary preadipocytes were isolated as described previously (Hausman et al., 2008). Briefly, the white adipose pads were removed from *Lmna*$^{-/-}$ mice and finely minced in DMEM/F12 medium. The minced tissues were incubated with 4-(2-hydroxyethyl)-1-piperazineethanesulfonic acid (HEPES):collagenase solution (collagenase type 1, Worthington Biochemical, LS004196) for 45 min in a shaking water bath at 37°C. When digestion was completed, additional DMEM/F12 medium was added, and the whole solution was filtered through a 240-μm mesh filter. The digested fat solution was centrifuged and resuspended with red blood cell (RBC) lysis solution for 5 min to remove the blood cells. The preadipocytes were plated with plating medium (DMEM/F12 + 10% FBS) under normal culture conditions (37°C, 5% CO_2) for 3 days before DMSO or rapamycin (100 nM) treatment. Cell lysates were collected for immunoblotting. For isolation of preadipocytes from BAT, a similar strategy was used but with collagenase type A (Worthington Biochemical, LS004152) in DMEM instead (Fasshauer et al., 2001).

Statistical Analysis

All statistical analyses were conducted using GraphPad Prism 6 (GraphPad). The survival curves were completed using a Kaplan-Meier curve. We used a log-rank (Mantel-Cox) test to perform the statistical analyses of the survival curves. All the other data are shown as mean ± SEM. The statistical significance of differences between two groups was determined using unpaired, two-tailed Student's t test (*$p < 0.05$).

SUPPLEMENTAL INFORMATION

Supplemental Information includes five figures and can be found with this article online at http://dx.doi.org/10.1016/j.celrep.2016.10.040.

AUTHOR CONTRIBUTIONS

C.Y.L., B.K.K., Y.M.H., M.N.O., and M.A.M. participated in the design of parts of the experiments. C.Y.L., S.S.A., N.H.C., J.R.M., E.C.A., M.N.O., J.A.W., C.P., M.A.T., E.P.L., Y.M.H., and D.M.M. performed the experiments. C.Y.L. analyzed the data. C.Y.L. and B.K.K. wrote the manuscript with input from the co-authors.

ACKNOWLEDGMENTS

We would like to thank the vivarium staff at the Buck Institute for Research on Aging for their expert treatment and monitoring of the mice. This work was funded by the National Institute on Aging (R01 AG033373 and R01 AG024287 (to B.K.K.). C.Y.L. is supported by a Glenn/AFAR postdoctoral fellowship. B.K.K. is an Ellison Medical Foundation Senior Scholar in Aging.

Received: March 16, 2016
Revised: July 27, 2016
Accepted: October 13, 2016
Published: December 6, 2016

REFERENCES

Albert, V., and Hall, M.N. (2015). mTOR signaling in cellular and organismal energetics. Curr. Opin. Cell Biol. *33*, 55–66.

Anisimov, V.N., Zabezhinski, M.A., Popovich, I.G., Piskunova, T.S., Semenchenko, A.V., Tyndyk, M.L., Yurova, M.N., Rosenfeld, S.V., and Blagosklonny, M.V. (2011). Rapamycin increases lifespan and inhibits spontaneous tumorigenesis in inbred female mice. Cell Cycle *10*, 4230–4236.

Arimura, T., Helbling-Leclerc, A., Massart, C., Varnous, S., Niel, F., Lacène, E., Fromes, Y., Toussaint, M., Mura, A.M., Keller, D.I., et al. (2005). Mouse model carrying H222P-Lmna mutation develops muscular dystrophy and dilated cardiomyopathy similar to human striated muscle laminopathies. Hum. Mol. Genet. *14*, 155–169.

Cai, H., Dong, L.Q., and Liu, F. (2016). Recent Advances in Adipose mTOR Signaling and Function: Therapeutic Prospects. Trends Pharmacol. Sci. *37*, 303–317.

Chakrabarti, P., English, T., Shi, J., Smas, C.M., and Kandror, K.V. (2010). Mammalian target of rapamycin complex 1 suppresses lipolysis, stimulates lipogenesis, and promotes fat storage. Diabetes *59*, 775–781.

Chakrabarti, P., Kim, J.Y., Singh, M., Shin, Y.K., Kim, J., Kumbrink, J., Wu, Y., Lee, M.J., Kirsch, K.H., Fried, S.K., and Kandror, K.V. (2013). Insulin inhibits lipolysis in adipocytes via the evolutionarily conserved mTORC1-Egr1-ATGL-mediated pathway. Mol. Cell. Biol. *33*, 3659–3666.

Choi, J.C., Muchir, A., Wu, W., Iwata, S., Homma, S., Morrow, J.P., and Worman, H.J. (2012). Temsirolimus activates autophagy and ameliorates cardiomyopathy caused by lamin A/C gene mutation. Sci. Transl. Med. *4*, 144ra102.

Cutler, D.A., Sullivan, T., Marcus-Samuels, B., Stewart, C.L., and Reitman, M.L. (2002). Characterization of adiposity and metabolism in Lmna-deficient mice. Biochem. Biophys. Res. Commun. *291*, 522–527.

Fang, Y., Westbrook, R., Hill, C., Boparai, R.K., Arum, O., Spong, A., Wang, F., Javors, M.A., Chen, J., Sun, L.Y., and Bartke, A. (2013). Duration of rapamycin treatment has differential effects on metabolism in mice. Cell Metab. *17*, 456–462.

Fasshauer, M., Klein, J., Kriauciunas, K.M., Ueki, K., Benito, M., and Kahn, C.R. (2001). Essential role of insulin receptor substrate 1 in differentiation of brown adipocytes. Mol. Cell. Biol. *21*, 319–329.

Fedorenko, A., Lishko, P.V., and Kirichok, Y. (2012). Mechanism of fatty-acid-dependent UCP1 uncoupling in brown fat mitochondria. Cell *151*, 400–413.

Fischer, K.E., Gelfond, J.A., Soto, V.Y., Han, C., Someya, S., Richardson, A., and Austad, S.N. (2015). Health Effects of Long-Term Rapamycin Treatment: The Impact on Mouse Health of Enteric Rapamycin Treatment from Four Months of Age throughout Life. PLoS ONE *10*, e0126644.

Fong, L.G., Frost, D., Meta, M., Qiao, X., Yang, S.H., Coffinier, C., and Young, S.G. (2006). A protein farnesyltransferase inhibitor ameliorates disease in a mouse model of progeria. Science *311*, 1621–1623.

Fujishita, T., Aoki, K., Lane, H.A., Aoki, M., and Taketo, M.M. (2008). Inhibition of the mTORC1 pathway suppresses intestinal polyp formation and reduces mortality in ApcDelta716 mice. Proc. Natl. Acad. Sci. USA *105*, 13544–13549.

Haemmerle, G., Lass, A., Zimmermann, R., Gorkiewicz, G., Meyer, C., Rozman, J., Heldmaier, G., Maier, R., Theussl, C., Eder, S., et al. (2006). Defective lipolysis and altered energy metabolism in mice lacking adipose triglyceride lipase. Science *312*, 734–737.

Harrison, D.E., Strong, R., Sharp, Z.D., Nelson, J.F., Astle, C.M., Flurkey, K., Nadon, N.L., Wilkinson, J.E., Frenkel, K., Carter, C.S., et al. (2009). Rapamycin fed late in life extends lifespan in genetically heterogeneous mice. Nature *460*, 392–395.

Hausman, D.B., Park, H.J., and Hausman, G.J. (2008). Isolation and culture of preadipocytes from rodent white adipose tissue. Methods Mol. Biol. *456*, 201–219.

Jahn, D., Schramm, S., Schnölzer, M., Heilmann, C.J., de Koster, C.G., Schütz, W., Benavente, R., and Alsheimer, M. (2012). A truncated lamin A in the Lmna -/- mouse line: implications for the understanding of laminopathies. Nucleus *3*, 463–474.

Johnson, S.C., Rabinovitch, P.S., and Kaeberlein, M. (2013a). mTOR is a key modulator of ageing and age-related disease. Nature *493*, 338–345.

Johnson, S.C., Yanos, M.E., Kayser, E.B., Quintana, A., Sangesland, M., Castanza, A., Uhde, L., Hui, J., Wall, V.Z., Gagnidze, A., et al. (2013b). mTOR inhibition alleviates mitochondrial disease in a mouse model of Leigh syndrome. Science *342*, 1524–1528.

Julien, L.A., Carriere, A., Moreau, J., and Roux, P.P. (2010). mTORC1-activated S6K1 phosphorylates Rictor on threonine 1135 and regulates mTORC2 signaling. Mol. Cell. Biol. *30*, 908–921.

Kumar, A., Lawrence, J.C., Jr., Jung, D.Y., Ko, H.J., Keller, S.R., Kim, J.K., Magnuson, M.A., and Harris, T.E. (2010). Fat cell-specific ablation of rictor in mice impairs insulin-regulated fat cell and whole-body glucose and lipid metabolism. Diabetes *59*, 1397–1406.

Lamming, D.W., and Sabatini, D.M. (2013). A Central role for mTOR in lipid homeostasis. Cell Metab. *18*, 465–469.

Lamming, D.W., Ye, L., Katajisto, P., Goncalves, M.D., Saitoh, M., Stevens, D.M., Davis, J.G., Salmon, A.B., Richardson, A., Ahima, R.S., et al. (2012). Rapamycin-induced insulin resistance is mediated by mTORC2 loss and uncoupled from longevity. Science *335*, 1638–1643.

Laplante, M., and Sabatini, D.M. (2012). mTOR signaling in growth control and disease. Cell *149*, 274–293.

Liu, B., Ghosh, S., Yang, X., Zheng, H., Liu, X., Wang, Z., Jin, G., Zheng, B., Kennedy, B.K., Suh, Y., et al. (2012). Resveratrol rescues SIRT1-dependent adult stem cell decline and alleviates progeroid features in laminopathy-based progeria. Cell Metab. *16*, 738–750.

Liu, Y., Diaz, V., Fernandez, E., Strong, R., Ye, L., Baur, J.A., Lamming, D.W., Richardson, A., and Salmon, A.B. (2014). Rapamycin-induced metabolic defects are reversible in both lean and obese mice. Aging (Albany, N.Y.) *6*, 742–754.

Lopez-Mejia, I.C., de Toledo, M., Chavey, C., Lapasset, L., Cavelier, P., Lopez-Herrera, C., Chebli, K., Fort, P., Beranger, G., Fajas, L., et al. (2014). Antagonistic functions of LMNA isoforms in energy expenditure and lifespan. EMBO Rep. *15*, 529–539.

Mariño, G., Ugalde, A.P., Fernández, A.F., Osorio, F.G., Fueyo, A., Freije, J.M., and López-Otín, C. (2010). Insulin-like growth factor 1 treatment extends longevity in a mouse model of human premature aging by restoring somatotroph axis function. Proc. Natl. Acad. Sci. USA *107*, 16268–16273.

Miller, R.A., Harrison, D.E., Astle, C.M., Fernandez, E., Flurkey, K., Han, M., Javors, M.A., Li, X., Nadon, N.L., Nelson, J.F., et al. (2014). Rapamycin-mediated lifespan increase in mice is dose and sex dependent and metabolically distinct from dietary restriction. Aging Cell *13*, 468–477.

Neff, F., Flores-Dominguez, D., Ryan, D.P., Horsch, M., Schröder, S., Adler, T., Afonso, L.C., Aguilar-Pimentel, J.A., Becker, L., Garrett, L., et al. (2013). Rapamycin extends murine lifespan but has limited effects on aging. J. Clin. Invest. *123*, 3272–3291.

Nikolova, V., Leimena, C., McMahon, A.C., Tan, J.C., Chandar, S., Jogia, D., Kesteven, S.H., Michalicek, J., Otway, R., Verheyen, F., et al. (2004). Defects in nuclear structure and function promote dilated cardiomyopathy in lamin A/C-deficient mice. J. Clin. Invest. *113*, 357–369.

Osorio, F.G., Navarro, C.L., Cadiñanos, J., López-Mejía, I.C., Quirós, P.M., Bartoli, C., Rivera, J., Tazi, J., Guzmán, G., Varela, I., et al. (2011). Splicing-directed therapy in a new mouse model of human accelerated aging. Sci. Transl. Med. *3*, 106ra107.

Peinado, J.R., Quiros, P.M., Pulido, M.R., Marino, G., Martinez-Chantar, M.L., Vazquez-Martinez, R., Freije, J.M., Lopez-Otin, C., and Malagon, M.M. (2011). Proteomic profiling of adipose tissue from Zmpste24−/− mice, a model of lipodystrophy and premature aging, reveals major changes in mitochondrial function and vimentin processing. Mol. Cell Proteomics *10*, M111 008094.

Polak, P., Cybulski, N., Feige, J.N., Auwerx, J., Rüegg, M.A., and Hall, M.N. (2008). Adipose-specific knockout of raptor results in lean mice with enhanced mitochondrial respiration. Cell Metab. *8*, 399–410.

Ramos, F.J., Chen, S.C., Garelick, M.G., Dai, D.F., Liao, C.Y., Schreiber, K.H., MacKay, V.L., An, E.H., Strong, R., Ladiges, W.C., et al. (2012). Rapamycin reverses elevated mTORC1 signaling in lamin A/C-deficient mice, rescues cardiac and skeletal muscle function, and extends survival. Sci. Transl. Med. *4*, 144ra103.

Sarbassov, D.D., Ali, S.M., Sengupta, S., Sheen, J.H., Hsu, P.P., Bagley, A.F., Markhard, A.L., and Sabatini, D.M. (2006). Prolonged rapamycin treatment inhibits mTORC2 assembly and Akt/PKB. Mol. Cell *22*, 159–168.

Schreiber, K.H., and Kennedy, B.K. (2013). When lamins go bad: nuclear structure and disease. Cell *152*, 1365–1375.

Schreiber, K.H., Ortiz, D., Academia, E.C., Anies, A.C., Liao, C.Y., and Kennedy, B.K. (2015). Rapamycin-mediated mTORC2 inhibition is determined by the relative expression of FK506-binding proteins. Aging Cell *14*, 265–273.

Schweiger, M., Schreiber, R., Haemmerle, G., Lass, A., Fledelius, C., Jacobsen, P., Tornqvist, H., Zechner, R., and Zimmermann, R. (2006). Adipose triglyceride lipase and hormone-sensitive lipase are the major enzymes in adipose tissue triacylglycerol catabolism. J. Biol. Chem. *281*, 40236–40241.

Sullivan, T., Escalante-Alcalde, D., Bhatt, H., Anver, M., Bhat, N., Nagashima, K., Stewart, C.L., and Burke, B. (1999). Loss of A-type lamin expression compromises nuclear envelope integrity leading to muscular dystrophy. J. Cell Biol. *147*, 913–920.

Ukropec, J., Anunciado, R.P., Ravussin, Y., Hulver, M.W., and Kozak, L.P. (2006). UCP1-independent thermogenesis in white adipose tissue of cold-acclimated Ucp1-/- mice. J. Biol. Chem. *281*, 31894–31908.

Worman, H.J., and Bonne, G. (2007). "Laminopathies": a wide spectrum of human diseases. Exp. Cell Res. *313*, 2121–2133.

Xiang, X., Lan, H., Tang, H., Yuan, F., Xu, Y., Zhao, J., Li, Y., and Zhang, W. (2015). Tuberous sclerosis complex 1-mechanistic target of rapamycin complex 1 signaling determines brown-to-white adipocyte phenotypic switch. Diabetes *64*, 519–528.

Zhang, H., Kieckhaefer, J.E., and Cao, K. (2013a). Mouse models of laminopathies. Aging Cell *12*, 2–10.

Zhang, Y., Bokov, A., Gelfond, J., Soto, V., Ikeno, Y., Hubbard, G., Diaz, V., Sloane, L., Maslin, K., Treaster, S., et al. (2013b). Rapamycin extends life and health in C57BL/6 mice. J. Gerontol. A Biol. Sci. Med. Sci. *69*, 119–130.